nature materials

ARTICLES

PUBLISHED ONLINE: 9 JANUARY 2011 | DOI: 10.1038/NMAT2930

A damage-tolerant glass

Marios D. Demetriou[1]*, Maximilien E. Launey[2†], Glenn Garrett[1], Joseph P. Schramm[1], Douglas C. Hofmann[1], William L. Johnson[1] and Robert O. Ritchie[2,3]

Owing to a lack of microstructure, glassy materials are inherently strong but brittle, and often demonstrate extreme sensitivity to flaws. Accordingly, their macroscopic failure is often not initiated by plastic yielding, and almost always terminated by brittle fracture. Unlike conventional brittle glasses, metallic glasses are generally capable of limited plastic yielding by shear-band sliding in the presence of a flaw, and thus exhibit toughness–strength relationships that lie between those of brittle ceramics and marginally tough metals. Here, a bulk glassy palladium alloy is introduced, demonstrating an unusual capacity for shielding an opening crack accommodated by an extensive shear-band sliding process, which promotes a fracture toughness comparable to those of the toughest materials known. This result demonstrates that the combination of toughness and strength (that is, damage tolerance) accessible to amorphous materials extends beyond the benchmark ranges established by the toughest and strongest materials known, thereby pushing the envelope of damage tolerance accessible to a structural metal.

Crystalline materials exhibit ordered structures with morphological features (for example, grains) that usually extend to the microscopic level. The defects associated with these microstructural features (for example, dislocations) become mobile under stress, enabling extensive plastic shielding ahead of an opening crack, which promotes high fracture toughness. The elastic-energy threshold for these defects to become active, however, is often low, resulting in rather low yield strengths. For example, ductile metals (for example, low-carbon steels) have very high fracture toughness ($>200\,\mathrm{MPa\,m^{1/2}}$), but a fairly low plastic yield strength ($<500\,\mathrm{MPa}$). By contrast, materials with amorphous atomic structures lacking microstructural defects could potentially yield plastically at much higher strengths. Because of the absence of these defects, however, the attainable plasticity ahead of an opening crack tip is limited, and consequently an opening failure is usually accommodated by unstable crack propagation, resulting in low fracture toughness and often low strength. For example, oxide glasses such as silicates have very high estimated yield strengths (up to 3 GPa) but lack any substantial toughness ($<1\,\mathrm{MPa\,m^{1/2}}$), and consequently their failure is accommodated by brittle fracture occurring well below the theoretical yield strength ($<100\,\mathrm{MPa}$). In this regard, the properties of toughness and strength are invariably mutually exclusive in essentially all classes of materials[1]. This inherent trade-off between strength and toughness is the fundamental challenge in the quest for highly damage-tolerant materials[2]. So far, some success has been achieved through development of composite microstructures, which typically combine a strong glassy matrix with ductile crystalline reinforcements at structural length scales that suppress fracture while maintaining high strength[3]. Achieving combinations of strength and toughness that fall outside the benchmarks of traditional structural metals, however, remains an outstanding challenge. In this article, a monolithic metallic glass alloy is introduced demonstrating a level of damage tolerance previously inaccessible to the toughest and strongest engineering materials known.

Unlike brittle oxide glasses, metallic glasses are generally likely to yield plastically under an opening stress. Consequently, most metallic glasses demonstrate substantial fracture toughness, and strengths consistent with the limit of elasticity of the amorphous structure (~2% of Young's modulus). Toughness–strength data reported so far for metallic glasses bridge the gap between brittle ceramics and marginally tough metals[4–6]. Specifically, reported fracture toughness values range from just over $1\,\mathrm{MPa\,m^{1/2}}$ (for brittle rare-earth and ferrous metal glasses)[7,8] to about $100\,\mathrm{MPa\,m^{1/2}}$ (for tougher noble- and early-transition-metal glasses)[9–11]. Reported strengths vary from about 0.5 GPa (for weak rare-earth metal glasses)[7] to as high as 5 GPa (for strong ferrous metal glasses)[12]. As demonstrated here, the toughness potentially accessible to an amorphous metal in fact extends much further, approaching values characteristic of the toughest materials known, while strengths consistent with the elasticity of the amorphous structure are retained.

Mechanistically, when an opening stress of the order of the material yield strength is applied, plastic shear sliding ensues, confined within nanoscopic bands (shear bands) oriented along planes of maximum resolved shear stress. Such shear bands propagate by slip under negative pressure up to some critical shear strain, beyond which they evolve into opening cracks. Under uniform negative pressure, as in quasi-static uniaxial tension, shear band opening in bulk samples becomes unstable and a crack propagates rapidly across the glassy structure, resulting in essentially zero macroscopic plastic strain. In a quasi-stable loading geometry, however, as in bending, shear sliding initiated at the tensile surface can be arrested if propagated to the neutral axis without opening, such that stable plastic deformation can be achieved[13]. Atomistically, local shear sliding in the shear band is accommodated by cooperative inelastic rearrangements of local clusters of ~100 atoms[14]. Shearing can be sustained under negative pressure until low-density configurations develop and critical cavities eventually emerge. On the intervention of cavitation, plastic

[1]Keck Engineering Laboratories, California Institute of Technology, Pasadena, California 91125, USA, [2]Materials Sciences Division, Lawrence Berkeley National Laboratory, Berkeley, California 94720, USA, [3]Department of Materials Science and Engineering, University of California, Berkeley, California 94720, USA. †Present address: Cordis Corporation, a Johnson & Johnson Company, 6500 Paseo Padre Parkway, Fremont, California 94555, USA.
*e-mail: marios@caltech.edu.

shearing is terminated and mechanical energy is dissipated through crack extension[15]. We can therefore expect that the extent to which a glass can undergo shear sliding under negative pressure before forming critical cavities should be proportional to its capacity to plastically shield an opening crack, and by extension to its overall fracture toughness. It is therefore conceivable that very large fracture toughness values are theoretically possible for glasses with a capacity to undergo multiple configurational shear rearrangements before forming critical cavities, or equivalently with activation barriers for shear flow much smaller than the activation barriers for cavitation. The glassy metal introduced here seems to exhibit such capacity, as it demonstrates an unusual propensity for shear flow without cavitation, which promotes very high fracture toughness.

Bulk-glass formation in Pd-rich metal–metalloid composition space is explored in the current work. The glass-forming ability of Pd–metalloid systems was first recognized by Duwez *et al.* in 1969 (ref. 16). Early Pd-rich metal–metalloid systems demonstrated only marginal glass-forming ability, but exhibited a very high Poisson ratio (approaching 0.42; ref. 17) together with a high glass-transition temperature (in excess of 600 K; ref. 18); high values for these two properties, as we argue later in the article, designate a high glass toughness. Indeed, a fairly robust fracture resistance was noted for these early marginal glass formers[19,20]. In the present study, Pd-rich metal–metalloid compositions were sought capable of forming bulk glasses and exhibiting Poisson ratios and glass-transition temperatures comparable to those of the early glass formers.

Here, the combination of Pd with P, Si and Ge at composition $Pd_{82.5}P_6Si_{9.5}Ge_2$ (at.%) was found capable of forming glassy rods 1 mm in diameter. Microalloying this composition with Ag was found to dramatically enhance glass formation. Specifically, alloy $Pd_{79}Ag_{3.5}P_6Si_{9.5}Ge_2$ was found capable of forming glassy rods 6 mm in diameter. X-ray diffraction, high-resolution transmission electron microscopy and differential scanning calorimetry analyses verifying the amorphous structure of the $Pd_{79}Ag_{3.5}P_6Si_{9.5}Ge_2$ glass are presented in Fig. 1. A glass-transition temperature of 613 K is observed in the thermal scan. Using ultrasonic measurements, the bulk and shear moduli were measured to be 172 GPa and 31 GPa, respectively, with a Poisson ratio of ~0.42. A representative loading curve obtained for a bulk specimen loaded quasi-statically in tension is presented in Fig. 2a, with corresponding micrographs of the fracture surface in Fig. 2b. The tensile loading response seems to depart from linear elasticity and, on yielding, several slip events are evident (see the inset in Fig. 2a). The stress of 1,490 MPa marking the first slip event is taken to represent the material plastic yield strength σ_y. Interestingly, a small total plastic strain of ~0.15% was recorded. The corresponding fracture surface (Fig. 2b) is non-planar, revealing multiple failure planes (facets) and a large crack offset that did not extend across the gauge section. A ~40-μm-wide shear offset is apparent, revealing evidence of extensive 'stair-like' plastic sliding before fracture. These features, which are unusual for tensile failure of a monolithic glass, are consistent with the evidence of limited plasticity recorded in the loading curve. In the absence of a microstructural stabilizing mechanism, however, the attained plasticity cannot properly be termed 'ductility'; rather, this extensive multiplane sliding activity is a demonstration of very high glass toughness.

Assessing the fracture toughness of metallic glasses showing extensive plasticity can be extremely challenging, because meeting the fracture-mechanics requirements for linear-elastic K-field dominance and the development of plane-strain conditions demand specimen sizes that often exceed the critical thickness for glass formation. For example, measurement of a linear-elastic fracture toughness K_{Ic} value of 200 MPa $m^{1/2}$ (K_{Ic} is the critical

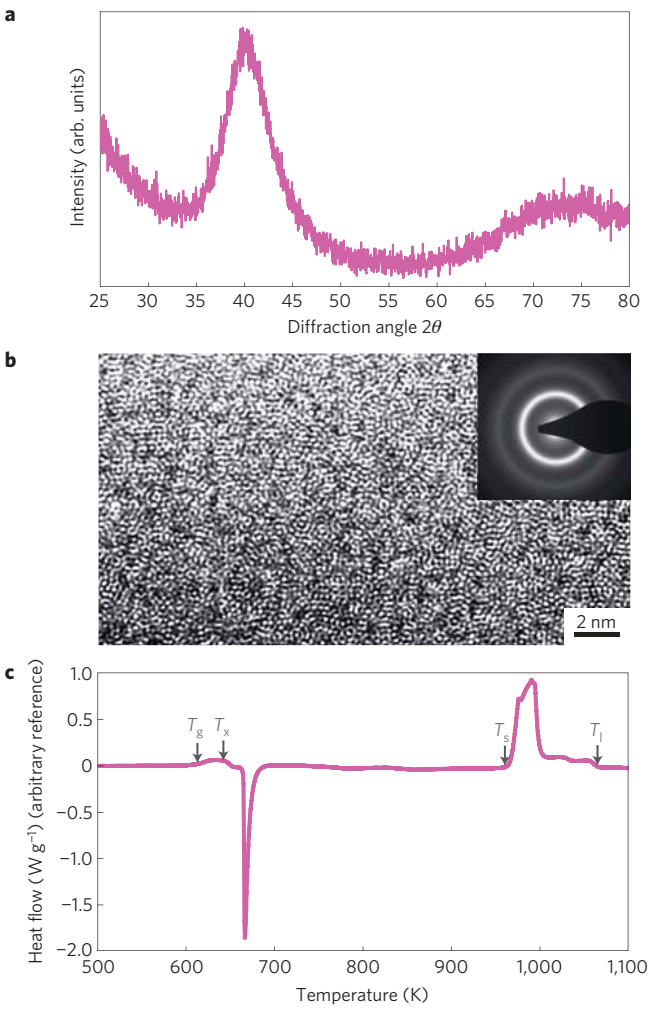

Figure 1 | Amorphous structure of the $Pd_{79}Ag_{3.5}P_6Si_{9.5}Ge_2$ glass. a, X-ray diffraction analysis, **b**, high-resolution transmission electron microscopy and **c**, differential scanning calorimetry of a bulk $Pd_{79}Ag_{3.5}P_6Si_{9.5}Ge_2$ glassy sample. Arrows in **c** indicate the glass-transition temperature $T_g = 613$ K, the crystallization temperature $T_x = 644$ K, the solidus temperature $T_s = 967$ K and the liquidus temperature $T_l = 1{,}065$ K.

value of the stress intensity K at crack initiation, or at fracture instability) requires sample dimensions (in terms of crack size, ligament depth and thickness) in excess of 45 mm to be considered valid; such dimensions exceed the critical casting thickness of even robust metallic bulk-glass formers. Although single-value toughness measurements such as K_{Ic} properly define the toughness for crack initiation in brittle materials, they are not always sufficient to characterize the toughness of glassy metals demonstrating extensive plastic yielding, or exhibiting toughening mechanisms that result in significant subcritical crack growth before unstable fracture[21]. To overcome the size constraints for meeting the small-scale yielding conditions while still properly accounting for the extension of the crack, we here implement a crack-tip opening displacement (CTOD) approach. Specifically, the relationship between the J-integral, that is, the nonlinear strain-energy release rate, and δ_t, the CTOD, is used, given by $J = d_n\sigma_0\delta_t$, where σ_0 is the flow stress (the average of the yield and ultimate stresses) and d_n is a constant tabulated from the strain-hardening exponent, n, of the material (see Supplementary Discussion for more details on the CTOD approach)[22–24]. A finite n is essential for the J-field to dominate over some finite region ahead of a crack tip. Glassy $Pd_{79}Ag_{3.5}P_6Si_{9.5}Ge_2$ shows a small degree of apparent hardening in

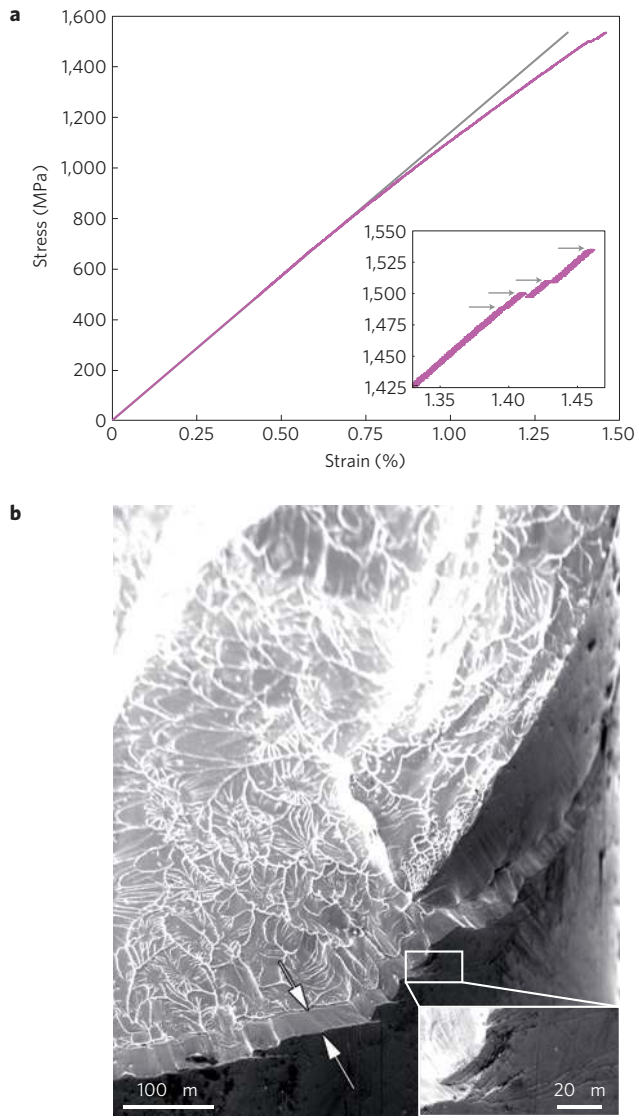

Figure 2 | Tensile test of the $Pd_{79}Ag_{3.5}P_6Si_{9.5}Ge_2$ glass. a, Tensile loading curve of a bulk glassy $Pd_{79}Ag_{3.5}P_6Si_{9.5}Ge_2$ specimen. The grey line is a guide for linear elastic response. Inset: Magnified view of the loading curve in the vicinity of yielding. Arrows indicate multiple slip events recorded before fracture. **b**, Micrograph of the fracture-surface morphology. White arrows designate the shear-sliding offset width. Inset: Magnified view in the vicinity of a shear step, revealing dense shear-band activity.

bending (attributed mostly to multiplication and intersection of shear bands giving rise to local compatibility stresses) such that $n \approx 0.13$ (see Supplementary Discussion and Supplementary Figs S1 and S2), thus ensuring that the J-field crack-tip uniqueness is preserved. To verify that this approach is suitable for metallic glasses that undergo extensive plastic yielding, we compared fracture toughness values determined using the CTOD method with direct measurements of J-integral toughness for a ductile-phase-reinforced metallic glass, also exhibiting extensive plasticity. Good agreement was obtained between the two measurement techniques (see Supplementary Discussion and Supplementary Fig. S3).

Accordingly, we have used the CTOD approach to determine the fracture toughness of a metallic glass with critical casting thickness below the width required for direct J-integral toughness measurements. The mode-I (tensile-opening) fracture toughness of glassy $Pd_{79}Ag_{3.5}P_6Si_{9.5}Ge_2$ was determined in the single-edge/notched-beam bending, SE(B), geometry, using micronotched beams. Evaluation of toughness requires nonlinear elastic fracture mechanics to characterize contributions from plasticity and, more importantly, resistance-curve (R-curve) analysis to characterize the toughness associated with crack growth, both of which are afforded by the use of the δ_t–R curve (Fig. 3a). Results for the stress intensity K_J back-calculated from the J measurements are shown in Fig. 3b. The glass demonstrates extensive rising R-curve behaviour indicative of stable crack growth over hundreds of micrometres. A near-steady-state fracture toughness measured in terms of a stress intensity, K_{Jc}, of $\sim$200 MPa m$^{1/2}$ (or in terms of the J integral, $J_C \sim 460$ kJ m^{-2}) is attained. This is an exceptionally high value for any material, but especially for an inherently non-ductile solid with an entirely amorphous structure. More interestingly, the rising R-curve (Fig. 3b) indicates that the glass toughens as a crack extends: an attribute of ductile crystalline metals not previously thought possible for an amorphous material.

Mechanistically, we identified the salient sources of toughening in the glass by carrying out the fracture-toughness tests *in situ* in the scanning electron microscope. This technique enables the quantitative measurement of the R curve while simultaneously monitoring the evolution of damage ahead of the crack tip and the toughening mechanisms in the crack wake. The high toughness value is achieved by stabilizing the plastic-flow processes at the opening crack tip to form a distributed damage zone accompanied by significant plastic shielding (see Fig. 3c–k and Supplementary Movie). The specific mechanisms contributing to the toughness of the $Pd_{79}Ag_{3.5}P_6Si_{9.5}Ge_2$ glass can be described in terms of a three-step process. First, shear bands form along the fan-shaped (Prandtl-field) slip lines[25,26] that bend back toward the crack plane (Fig. 3d–f). Accompanying the development of the Prandtl field, extensive localized shear sliding occurs along the evolved slip planes, leading to very large shear offsets (Fig. 3f,g). When a critical sliding strain is reached with increasing load, an extended shear band opens at the notch tip and evolves as crack (Fig. 3g,h). Extensive shear banding is seen to persist ahead of the evolved crack tip, however, promoting significant crack-tip blunting (Fig. 3h,i). As the slip bands bend back to the crack plane, enabling substantial shear sliding, the crack remains stable on its plane such that stable crack extension is attained during fracture (Fig. 3g–k). It should be noted that outright fracture never occurred in any of the specimens under the geometry and conditions considered here.

Even though the mechanisms controlling the plastic-zone development in the present glass are not fundamentally different than in other metallic glasses, the characteristic length scales associated with such development are considerably larger. The shear-sliding process under an opening stress, which constitutes the key mechanism of plastic-zone development, is illustrated schematically in Fig. 4a. Although all metallic glasses are generally capable of undergoing limited shear-band sliding in the presence of a flaw, the extent of shear sliding and observed shear offsets seen in the present glass are unprecedented. As shown in Fig. 4b, shear offsets as large as 50 μm are attained before crack opening. These extended offsets enable the build-up of a very large plastic zone; the homogeneous plane-stress plastic-zone radius of the $Pd_{79}Ag_{3.5}P_6Si_{9.5}Ge_2$ glass can be estimated to be as large as $r_p = K_c^2/\pi\sigma_y^2 \approx 6$ mm.

To investigate the self-similarity in plastic-zone development extending over several orders of magnitude in size for the various metallic-glass systems, a scaling law is introduced. The number of net activated shear-transformation events before a cavitation event in the core of an operating shear band is described here by a dimensionless parameter f, defined as $f = \exp[-(W_s - W_c)/k_BT]$, where W_s and W_c are the activation energy barriers for shear flow and cavitation respectively, and T is a reference temperature. The glass-transition temperature of the amorphous material is

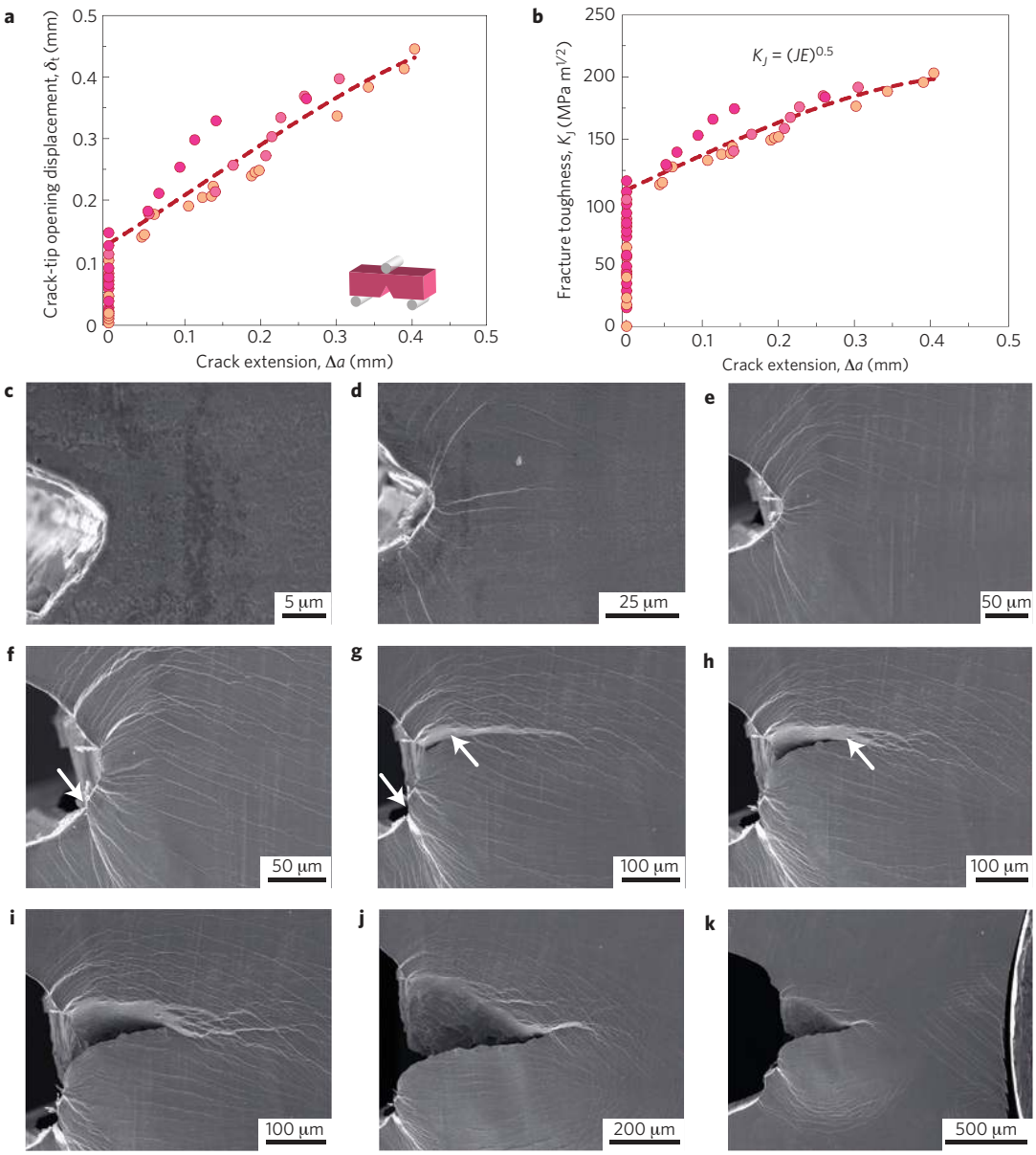

Figure 3 | Fracture toughness measurements of the $Pd_{79}Ag_{3.5}P_6Si_{9.5}Ge_2$ glass. a, The crack-tip opening displacement, δ_t, determined graphically, is plotted against the crack extension, Δa. **b**, Fracture toughness, K_J, back-calculated from the *J*-integral, plotted against the crack extension, Δa. **c**–**k**, Scanning electron micrographs taken during an *in situ R*-curve measurement of an SE(B) specimen. The specimen initially contained a sharp notch with a root radius of ~5 μm. The crack-tip opening displacement was measured graphically at regular intervals. The corresponding fracture toughness K_J values are 0 MPa m$^{1/2}$ (**c**), 25 MPa m$^{1/2}$ (**d**), 44 MPa m$^{1/2}$ (**e**), 63 MPa m$^{1/2}$ (**f**), 115 MPa m$^{1/2}$ (**g**), 133 MPa m$^{1/2}$ (**h**), 144 MPa m$^{1/2}$ (**i**), 196 MPa m$^{1/2}$ (**j**) and 203 MPa m$^{1/2}$ (**k**). **d**,**e**, Shear bands initiate at relatively low stress intensity values along the Prandtl slip lines. **f**,**g**, An increase in K_J is recorded associated with extensive shear sliding, which creates large shear offsets (indicated by arrows) and promotes significant crack-tip blunting. **g**–**k**, At high stress, a crack initiates by opening of a shear band (indicated by arrows) and subsequently extends at a stable rate. **k**, State of the specimen at the end of the test, showing that the sample did not fracture catastrophically after undergoing the entire strain applicable by the fixture.

recognized to be a good measure of the shear-flow barrier; specifically, $W_s \approx 37\,k_B T_g$ (refs 14,27,28). By further assuming that the ratio of the barrier heights W_c/W_s is dominated by the ratio of the respective elastic curvatures B/G, where B and G are the bulk and shear modulus respectively, we can arrive at the following relation for f:

$$\log(f) \sim \frac{W_s}{k_B T}\left(\frac{W_c}{W_s} - 1\right) \sim \frac{T_g}{T}\left(\frac{B}{G} - 1\right) \qquad (1)$$

Interestingly, the ratio of bulk to shear modulus B/G (or equivalently, the Poisson ratio) has been previously identified to be a key parameter associated with the toughness of a metallic glass[5,9]. This ratio alone, however, is not adequate to describe the number of net activated-shear events, as it does not take into account the absolute magnitude of the activation barriers (here approximated as $\sim k_B T_g$). Using equation (1), f is estimated for a set of ten metallic-glass alloys (including the present one) with toughness values that vary over two orders of magnitude (see Supplementary Discussion for the complete set of data). The estimated f for the present glass is found to be higher than the other glasses, consistent with its larger plastic zone and higher toughness. In fact f, which is formulated to describe the capacity for shear flow before cavitation, is found to show a one-to-one correspondence with r_p.

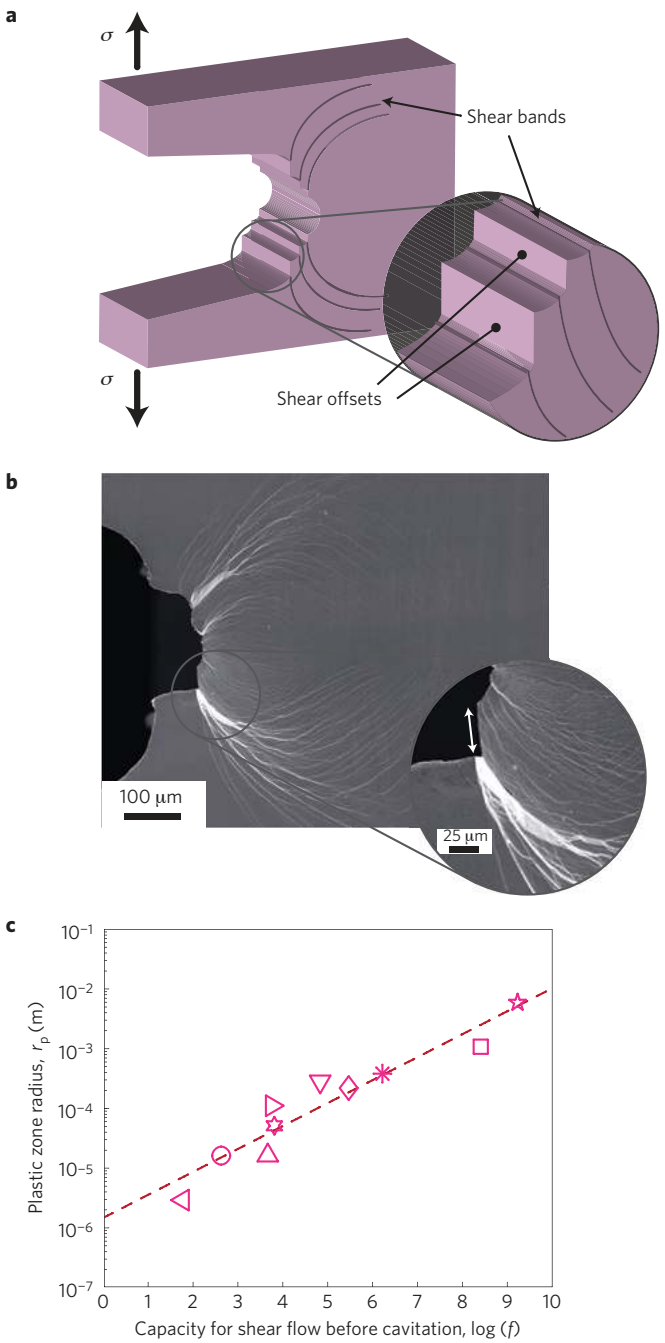

Figure 4 | Shear-sliding mechanism governing metallic-glass toughness. **a**, Schematic diagram illustrating the process of crack blunting through shear sliding in the vicinity of a flaw under opening stress. **b**, Micrograph of a deformed notch in a glassy $Pd_{79}Ag_{3.5}P_6Si_{9.5}Ge_2$ specimen showing extensive plastic shielding of an initially sharp crack. Inset: Magnified view revealing a 50-μm shear offset (arrow) developed during plastic sliding before the onset of crack opening. **c**, Logarithm of the plastic-zone radius, defined as $K_c^2/\pi\sigma_y^2$, plotted against the estimated capacity for shear flow before cavitation, approximated by $-(W_s - W_c)/k_BT$ (equation (1)). Data for ten metallic glass alloys are plotted (see Supplementary Discussion for the complete set of data and references). Symbols designate the following alloys: left triangle, $Mg_{65}Cu_{25}Tb_{10}$; circle, $La_{55}Al_{25}Ni_5Cu_{10}Co_5$; up triangle, $Fe_{58}Co_{6.5}Mo_{14}C_{15}B_6Er_{0.5}$; six-pointed star, $Fe_{66}Cr_3Mo_{10}C_{10}B_3P_8$; right triangle, $Fe_{70}Ni_5Mo_5C_5B_{2.5}P_{12.5}$; diamond, $Zr_{55}Cu_{30}Ni_5Al_{10}$; down triangle, $Zr_{41.2}Ti_{13.8}Cu_{12.5}Ni_{10}Be_{22.5}$; asterisk, $Cu_{60}Zr_{20}Hf_{10}Ti_{10}$; square, $Pt_{57.5}Cu_{14.7}Ni_{5.3}P_{22.5}$; five-pointed star, $Pd_{79}Ag_{3.5}P_6Si_{9.5}Ge_2$. The line is a regression to the data.

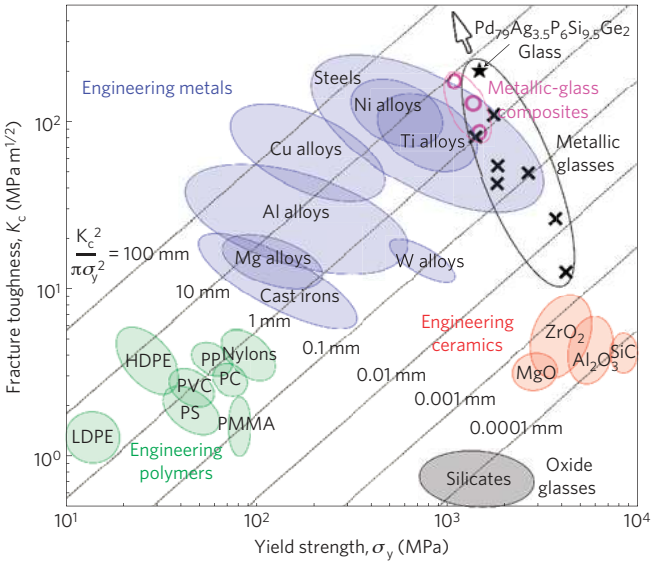

Figure 5 | Ashby map of the damage tolerance (toughness versus strength) of materials. Ranges of fracture toughness versus yield strength are shown for oxide glasses[29], engineering ceramics[29], engineering polymers[29] and engineering metals[29], along with data for the $Pd_{79}Ag_{3.5}P_6Si_{9.5}Ge_2$ glass designated by a filled star, data for other metallic glasses (three Fe-based glasses[30,31]; two Zr-based glasses[32,33]; a Ti-based glass[11] and a Pt-based glass[9]) designated by crosses and data for ductile-phase-reinforced metallic glasses[3] designated by circles. Yield-strength data shown for oxide glasses and ceramics represent ideal limits. Contours correspond to values for the plastic-zone radius, $K_c^2/\pi\sigma_y^2$. As indicated by the arrow, the combination of toughness and strength (that is, damage tolerance) potentially accessible to metallic glasses extends beyond traditional benchmarks towards levels previously inaccessible to any material.

As shown in Fig. 4c, parameter f correlates with r_p reasonably well, thereby describing the plastic-zone development in plastically yielding glasses over four orders of magnitude in size. On the basis of the correlation in Fig. 4c, we may conclude that the very high fracture resistance demonstrated by the present glass is attributable to a large absolute difference between W_s and W_c, as quantified by the high B/G and T_g values for this glass (equation (1)). Correspondingly, we believe that this scaling law with B, G and T_g as design variables (all of which are experimentally accessible) can serve as a viable guide for the development of a new generation of highly fracture-resistant structural glasses.

The values of fracture energy and toughness presented here for glassy $Pd_{79}Ag_{3.5}P_6Si_{9.5}Ge_2$ are comparable to values for the toughest engineering metals known (for example, low-carbon steels). Considering that a glass lacks microstructural defects such as dislocations, which rearrange to shield stress and suppress crack opening, achieving such high fracture resistance is quite remarkable. Moreover, in sharp contrast to tough crystalline metals, the absence of defects enables the very high strength associated with the amorphous structure. Thus, an unusual combination of very high strength and toughness (that is, very high damage tolerance) is possible—a feature perhaps unparalleled by any known monolithic material. In Fig. 5 we present an Ashby map[29] showing toughness-versus-strength ranges for oxide glasses, engineering ceramics, engineering polymers and engineering metals, along with data for monolithic metallic glasses (including the present glass) and ductile-phase-reinforced metallic glasses. As shown in the map, the toughness-versus-strength data for the present glass lie outside the benchmarks established by the strongest and toughest steels. In summary, the present results demonstrate that the

combination of toughness and strength (that is, the level of damage tolerance) potentially accessible to amorphous materials extends beyond the traditional limiting ranges towards levels previously inaccessible to any material.

Methods

Alloys were prepared by inductively melting pure elements in quartz tubes under inert atmosphere. Alloy ingots were fluxed with B_2O_3 at ~1,200 K for ~1,000 s. Glass formation was achieved by melting fluxed ingots in quartz tubes with 0.5-mm-thick walls and rapidly water-quenching. Amorphous tensile-test specimens were produced by water-quenching round tensile-bar-shaped quartz tubes containing the molten alloy. The specimen gauge sections were 1.5 mm in diameter and 20 mm in length. Tensile tests were carried out at room temperature and at a strain rate of 5×10^{-4} s^{-1}. SE(B) rectangular beam specimens for flexure measurements were prepared. The beam specimens had thickness 2.1 mm, width 2.1 mm, and length 20 mm. Fatigue precracking was rendered impractical here owing to the small size of the samples. Instead, a razor-micronotching technique was employed to generate a sharp crack within an acceptable range[34]. The notches were first introduced using a low-speed diamond saw, and then sharpened using a razor-micronotching technique. Micronotches with a root radius of ~5–10 μm were obtained by repeatedly sliding a razor blade over the saw-cut notch using a custom-made rig, while continually irrigating with a 1 μm diamond slurry. Sharp cracks with initial crack length of ~1.0 mm were generated. Before testing, specimens were polished to a 1 μm diamond suspension surface finish on both faces. Fracture-toughness tests were carried out *in situ* in a scanning electron microscope over a three-point bending stage.

Received 23 September 2010; accepted 19 November 2010; published online 9 January 2011

References

1. Launey, M. E. & Ritchie, R. O. On the fracture toughness of advanced materials. *Adv. Mater.* **21,** 2103–2110 (2009).
2. Ritchie, R. O. The quest for stronger, tougher materials. *Science* **320,** 448 (2008).
3. Hofmann, D. C. *et al.* Designing metallic glass matrix composites with high toughness and tensile ductility. *Nature* **451,** 1085–1089 (2008).
4. Ashby, M. F. & Greer, A. L. Metallic glasses as structural materials. *Scr. Mater.* **54,** 321–326 (2006).
5. Lewandowski, J. J. *et al.* Intrinsic plasticity or brittleness of metallic glasses. *Phil. Mag. Lett.* **85,** 77–87 (2005).
6. Xu, J. *et al.* The fracture toughness of bulk metallic glasses. *JOM* **62,** 10–18 (2010).
7. Xi, X. K. *et al.* Fracture of brittle metallic glasses: Brittleness or plasticity. *Phys. Rev. Lett.* **94,** 125510 (2005).
8. Hess, P. A. *et al.* Indentation fracture toughness of amorphous steel. *J. Mater. Res.* **20,** 783–786 (2005).
9. Schroers, J. & Johnson, W. L. Ductile bulk metallic glass. *Phys. Rev. Lett.* **93,** 255506 (2004).
10. Suh, J-Y. *et al.* Correlation between fracture surface morphology and toughness in Zr-based bulk metallic glasses. *J. Mater. Res.* **25,** 982–990 (2010).
11. Gu, X. J. *et al.* Compressive plasticity and toughness of a Ti-based bulk metallic glass. *Acta Mater.* **58,** 1708–1720 (2010).
12. Inoue, A. *et al.* Cobalt based bulk glassy alloy with ultrahigh strength and soft magnetic properties. *Nature Mater.* **2,** 661–663 (2003).
13. Conner, R. D. *et al.* Shear bands and cracking of metallic glass plates in bending. *J. Appl. Phys.* **94,** 904–911 (2003).
14. Johnson, W. L. & Samwer, K. A universal criterion for plastic yielding of metallic glasses with a $(T/T_g)^{2/3}$ temperature dependence. *Phys. Rev. Lett.* **95,** 195501 (2005).
15. Bouchaud, E. *et al.* Fracture through cavitation in a metallic glass. *Europhys. Lett.* **83,** 66006 (2008).
16. Duwez, P. *et al.* Amorphous phase in palladium–silicon alloys. *J. Appl. Phys.* **36,** 2267–2269 (1965).
17. Chen, H. S. *et al.* Elastic constants, hardness and their implications to flow properties of metallic glasses. *J. Non-Cryst. Solids* **18,** 157–171 (1975).
18. Chen, H. S. & Turnbull, D. Formation, stability, and structure of palladium–silicon based alloy glasses. *Acta Metall.* **17,** 1021–1031 (1969).
19. Kimura, H. & Masumoto, T. Deformation and fracture of an amorphous Pd–Cu–Si alloy in V-notch bending test. 1. Model mechanics of inhomogeneous plastic-flow in non-strain hardening solid. *Acta Metall.* **28,** 1663–1675 (1980).
20. Kimura, H. & Masumoto, T. Deformation and fracture of an amorphous Pd–Cu–Si alloy in V-notch bending test. 2. Ductile–brittle transition. *Acta Metall.* **28,** 1677–1693 (1980).
21. Launey, M. E. *et al.* Fracture toughness and crack resistance curve behavior in metallic glass matrix composites. *Appl. Phys. Lett.* **94,** 241910 (2009).
22. Shih, C. F. Relationships between the J-integral and the crack opening displacement for stationary and extending cracks. *J. Mech. Phys. Solids* **29,** 305–326 (1981).
23. Hutchinson, J. W. Plastic stress and strain fields at a crack tip. *J. Mech. Phys. Solids* **16,** 337–342 (1968).
24. Rice, J. R. & Rosengren, G. F. Plane strain deformation near a crack tip in a power-law hardening material. *J. Mech. Phys. Solids* **16,** 1–12 (1968).
25. Alpas, A. T. *et al.* Fracture and fatigue crack-propagation in a Ni-base metallic-glass. *Metall. Trans. A* **20,** 1395–1409 (1989).
26. Flores, K. M. & Dauskardt, R. H. Enhanced toughness due to stable crack tip damage zones in bulk metallic glass. *Scr. Mater.* **41,** 937–949 (1999).
27. Demetriou, M. D. *et al.* Cooperative shear model for the rheology of glass-forming metallic liquids. *Phys. Rev. Lett.* **97,** 065502 (2006).
28. Johnson, W. L. *et al.* Rheology and ultrasonic properties of metallic glass-forming liquids. *MRS Bull.* **32,** 644–650 (2007).
29. Ashby, M. F. *Materials Selection in Mechanical Design* (Pergamon, 1992).
30. Nouri, A. S. *et al.* Chemistry (intrinsic) and inclusion (extrinsic) effects on the toughness and Weibull modulus of Fe-based bulk metallic glasses. *Phil. Mag. Lett.* **88,** 853–861 (2008).
31. Demetriou, M. D. *et al.* Glassy steel optimized for glass-forming ability and toughness. *Appl. Phys. Lett.* **92,** 161910 (2008).
32. Kawashima, A. *et al.* Fracture toughness of $Zr_{55}Al_{10}Ni_5Cu_{30}$ bulk metallic glass by 3-point bend testing. *Mater. Trans.* **46,** 1725–1732 (2005).
33. Gilbert, C. J. *et al.* Fracture toughness and fatigue crack propagation in a Zr–Ti–Ni–Cu–Be bulk metallic glass. *Appl. Phys. Lett.* **71,** 476–478 (1997).
34. Lowhaphandu, P. & Lewandowski, J. J. Fracture toughness and notched toughness of bulk amorphous alloy: Zr–Ti–Ni–Cu–Be. *Scr. Mater.* **38,** 1811–1817 (1998).

Acknowledgements

M.D.D., G.G., J.P.S., D.C.H. and W.L.J. acknowledge support by the MRSEC program of the National Science Foundation under award number DMR-0520565 for the alloy development work. M.E.L. and R.O.R. acknowledge support by the Director, Office of Science, Office of Basic Energy Sciences, Division of Materials Sciences and Engineering, of the US Department of Energy under contract number DE-AC02-05CH11231 for the fracture-toughness characterization. The contributions of A. Wiest, J-Y. Suh, M. Floyd, C. Crewdson and C. Garland are also acknowledged.

Author contributions

M.D.D., M.E.L., W.L.J. and R.O.R. designed the research; M.D.D. developed the alloy; M.D.D., G.G., J.P.S. and D.C.H. characterized the alloy; M.E.L. carried out the mechanical testing; M.D.D., M.E.L., W.L.J. and R.O.R. wrote the manuscript.

Additional information

The authors declare no competing financial interests. Supplementary information accompanies this paper on www.nature.com/naturematerials. Reprints and permissions information is available online at http://npg.nature.com/reprintsandpermissions. Correspondence and requests for materials should be addressed to M.D.D.